Multi-Objective Optimization of Loading Paths for Double-Layered Tube Hydroforming using Finite Element Analysis

Hamed Ebrahimi Keshmarzi, Ramin Hashemi[*], Reza Madoliat

School of Mechanical Engineering,
Iran University of Science and Technology, Iran
E-mail: hamed.iust70@gmail.com, rhashemi@iust.ac.ir,
r_madoliat@iust.ac.ir
*Corresponding author

Abstract: One of the most important studies in tube hydroforming process is optimization of loading paths. The primary purpose of this research is to maximize formability by detecting the optimal forming parameters. The most significant settings in the prosperity of tube hydroforming process, are internal pressure and end axial feed (i.e., load path). In this paper, a finite element analysis was performed for a double-layered tube hydroforming process using the ABAQUS/Explicit software. Then, the finite element model has been verified with published experimental data. Using design of experiments (DOE) working with the Taguchi method, 32 loading paths are designed for optimization. All 32 loading paths are modelled using the finite element method in ABAQUS/Explicit and the magnitudes of bulge height and the total thickness of tubes at the branch tip are obtained in each loading path. The regression analysis is carried out to estimate the tubes formability and obtain objective functions that are bulge height and the total thickness of tubes at the protrusion peak as functions of loading parameters (internal pressure and axial feed). For solving the multi-objective optimization problem, the non-dominated sorting genetic algorithm II (NSGA-II) is utilized and the optimum results were obtained from the Pareto optimal front. Finally, the optimized loading path was applied to the finite element model and better formability (3.4% increase in the bulge height) has been achieved in the results.

Biographical notes: Hamed Ebrahimi Keshmarzi received his MSc in Mechanical Engineering from Iran University of Science and Technology. **Ramin Hashemi** is Associate Professor of Mechanical engineering at the Iran University of Science and Technology, Iran. His current research focuses on applied plasticity, metal forming and advanced engineering materials. **Reza Madoliat** is Associate Professor of Mechanical engineering at the Iran University of Science and Technology, Iran.

1   INTRODUCTION

Tube hydroforming (THF) is one of the unconventional manufacturing processes which is widely used to form complex shapes. Tube hydroforming offers several advantages over conventional manufacturing via stamping and welding, such as part consolidation, weight reduction, increasing in the strength and stiffness, enhanced uniform thickness distribution, decreasing of the work piece and tooling cost, etc. Because of this, in the past decades, researchers pay more attention to tube hydroforming [1-3]. In order to obtain the final favorable hydroformed tubes successfully, it is necessary to study the effect of process parameters on the results of forming. Loading Path is the most important parameter that actually is defined as how to apply internal pressure and axial feed during the forming process.

To achieve a satisfactory result, many "trial and error" runs may be needed. Clearly, the result gained from trial and error may not warranty a global optimum result. For this reason, several studies have expressed about optimization techniques combined with the finite element method (FEM) to specify the optimal loading conditions [4]. Double-Layered tubes are appropriate for the situations of severe corrosion and for chemical use in special circumferences (sea floor piping). The CRA-lined pipe (corrosion resistant alloy) is a well-known example of double-layered tubes that has been widely utilized in the refining industry, oil production and nuclear power plants [5-6].

Yingyot et al. studied two methods for optimization; self-feeding and adaptive simulation algorithms to identify the optimal loading conditions and experimental results were exhibited [7]. Aydemir et al. proposed an adaptive method to achieve a more efficient process control. This method avoids the onset of wrinkling and bursting via dedicated stability criteria [8]. Ingarao et al. offered an integration between numerical simulations, response surface method and Pareto optimal solution search techniques in order to design a complex Y-shaped tube hydroforming [9].

Abedrabbo et al. suggested a method to maximize formability by identifying the optimal loading condition using the Genetic algorithm by optimization software HEEDS combined with the nonlinear finite element code LS-DYNA [10]. Lorenzo et al. proposed an idea to integrate the steepest descent method with a moving least square approach in order to reach the optimal internal pressure curve in the hydroforming of a Y-shaped tube [11]. Kadkhodayan et al. determined the optimal loading condition using Simulated Annealing algorithm in conjunction with finite element analysis and analysis of variance [12]. Li et al. integrated an adaptive simulation approach with a fuzzy logic control algorithm [13].

Mirzaali et al. used Simulated Annealing algorithm which is directly incorporated into the non-linear finite element code ANSYS/LS-DYNA to analyse the forming parameters and obtain the optimal loading paths under a failure criterion based on the maximum allowable thinning and Von Mises stress [14]. Huang et al. introduced an adaptive support vector regression to determine the Pareto optimal solution set for T-shape tube hydroforming [4]. Ge et al. proposed a multi-objective optimization using differential evolution to obtain the optimum cooperation between the internal pressure and end feeding process [15].

Alaswad et al. modeled bulge height and wall thickness reduction of double-layered hydroformed tubes as functions of the geometrical factors using the combination of finite element analysis and response surface method for design of experiments and based on resultant models, a multi-response optimization study was conducted [16]. It can be seen from the literature review, there has been no report available regarding multi-objective optimization of the double-layered tube hydroforming to find the optimum loading path. In this paper, a multi-objective optimization method based on the non-dominated sorting genetic algorithm II (NSGA-II) is utilized.

For the first time, the multi-objective optimization of double-layered tube hydroforming process is investigated in the current research with an innovative approach in order to obtain loading paths design and make a mathematical relation between objective functions (bulge height and whole thickness at branch top) and loading parameters by considering process failures such as bursting and wrinkling. A finite element model is performed for double-layered tube hydroforming using ABAQUS/Explicit. After experimental verification, 30 loading variables and an appropriate period for each of them are designed. Based on these variables, using the design of experiments, 32 loading paths are specified. Oyane's ductile fracture criterion is utilized to avoid necking and bursting. Furthermore, a critical wrinkling stress is used to prevent buckling and wrinkling in the tube during the process. All 32 loading paths are simulated using the finite element method in ABAQUS/Explicit and the magnitudes of bulge height and whole thickness at branch top are obtained. Then the occurrence of the failure criteria consist of wrinkling and bursting is checked in each loading path.

If the failure occurs in one of the designed loading paths, that intended loading path is removed from the regression analysis. The regression analysis is performed to estimate objective functions. This novel procedure reduces the calculation costs and enhances the accuracy of estimated objective functions. NSGA-II Code, which is written in MATLAB, is used to solve the multi-objective optimization problem.

2   FINITE ELEMENT ANALYSIS

2.1. Finite Element Modelling

A precise modelling of the metal forming process using the finite element method is important in order to obtain accurate results. ABAQUS/Explicit is used to perform the finite element model of double-layered X-shape tube hydroforming ("Fig. 1"). Geometrical and Mechanical properties of two layers have been displayed in "Table 1 and Table 2". Internal pressure is considered 36 MPa and end axial feed is 12 mm. Reference [17] is used to verify the numerical simulation results with the experimental results and all geometrical and mechanical properties and loading conditions have been considered exactly same as the intended reference.
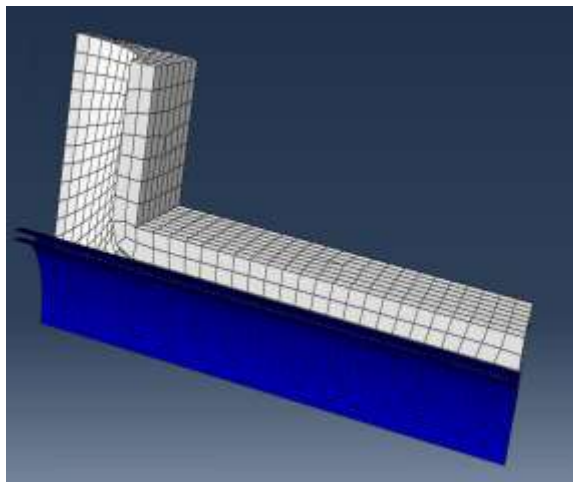

Fig. 1   Finite element modeling of double-layered X-shape tube hydroforming.

Table 1   The geometrical properties of two layers [17]

	Inner Layer	Outer Layer
Length (mm)	120	120
Inner Diameter (mm)	20.3	22
Outer Diameter (mm)	22	24

Table 2   The mechanical Properties of two layers [17]

Mechanical Properties	Inner Layer (Annealed Brass)	Outer Layer (Copper)
Density (gr/cc)	8.80	8.98
Elastic modulus (GPa)	100	105
Poisson's ratio	0.33	0.33
Yield stress (MPa)	98	220
Tangent modulus (MPa)	590	210

2.2. Experimental Verification

Olabi et al. conducted experiments on bi-layered tube hydroforming to form X-branch components from a combination of copper and annealed brass tubes [17]. To verify finite element results shown in "Fig. 2", the bulge height and total thickness at the branch tip have been compared with the published experimental data and was observed good agreement with experimental results ("Table 3").
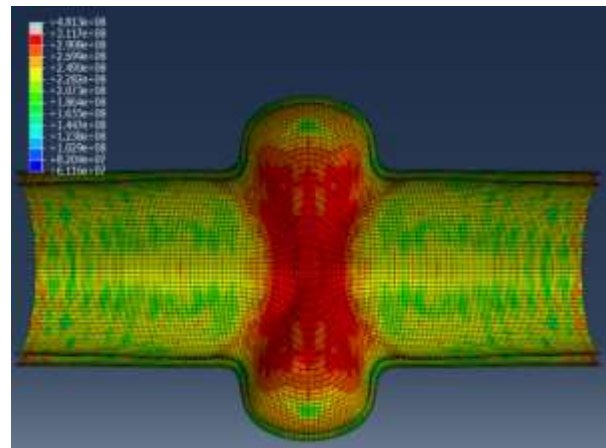

Fig. 2   Finite element Modelling results (Von Mises Stress Contour).

Table 3   Experimental and numerical results comparison

	Bulge height (mm)	Total thickness at branch tip (mm)
Experimental [17]	8.787	1.600
Numerical (Olabi) [17]	8.424	1.622
Numerical (Current research)	8.543	1.615
Error	2.77%	2.50%

3   OPTIMIZATION PROCEDURE

3.1. Definition of Initial Loading Paths

Loading path is defined as how to exert internal pressure and end axial feed versus process time. In order to determine the initial loading paths, the design of experiments (DOE) and Taguchi method is used.

The Taguchi method considers three stages in a process development: (1) system design (2) parameter design (3) tolerance design. Among these steps, parameter design is the most significant phase in the Taguchi method to obtain the best quality without cost increasing [18]. Therefore, in order to achieve the maximum formability, in the following, the parameter design approach by Taguchi method is performed.

Figure 3 depicts the internal pressure parameters and the time of each of them during the process. Also, the level of each parameter of internal pressure has been displayed in "Table 4".
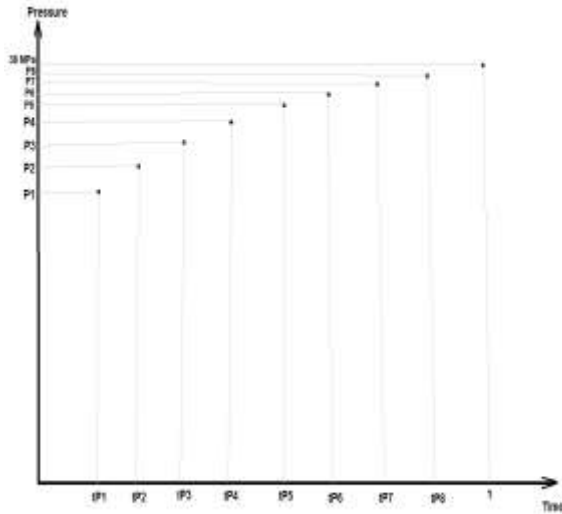
Fig. 3   The parameters of internal pressure during the process.

Table 3   The internal pressure parameters and their levels

Internal pressure	Level 1 Value (MPa)	Level 2 Value (MPa)	Internal pressure time	Level 1 Value (sec)	Level 2 Value (sec)
P1	30	34	tP1	0.01	0.11
P2	31	34	tP2	0.11	0.22
P3	32	34	tP3	0.22	0.33
P4	33	35	tP4	0.33	0.44
P5	34	35	tP5	0.44	0.55
P6	35	36	tP6	0.55	0.66
P7	35.5	36	tP7	0.66	0.77
P8	35.5	36	tP8	0.77	0.88

Figure 4 illustrates the axial feed parameters and the time of each of them during the process. Also, the level of each parameter of axial feed has been shown in "Table 5".
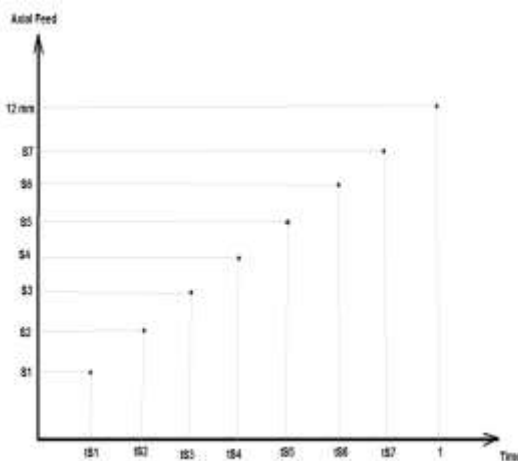

Fig. 4   The parameters of axial feed during the process.

Table 4   The axial feed parameters and their levels

Axial feed	Level 1 Value (mm)	Level 2 Value (mm)	Axial feed time	Level 1 Value (sec)	Level 2 Value (sec)
S1	1	3	tS1	0.01	0.125
S2	3	5	tS2	0.125	0.250
S3	5	7	tS3	0.250	0.375
S4	7	9	tS4	0.375	0.500
S5	9	10	tS5	0.500	0.625
S6	10	11	tS6	0.625	0.750
S7	11	12	tS7	0.750	0.875

Now, after determining parameters of internal pressure and axial feed, loading paths were designed using Taguchi method. Taguchi general form is as "Eq. (1)". In this equation, L is the symbol of Taguchi design, N is the number of experiments, k is the number of parameters and n is levels of each parameter [10].

$$L_N(n^k) \tag{1}$$

In the current study, Taguchi design is as "Eq. (2)". The mentioned design is carried out using statistical analysis by Minitab software.

$$L_{32}(2^{30}) \tag{2}$$

3.2. Failures in the Tube Hydroforming Process
One of the important goals of the tube hydroforming process is to obtain desirable products without defects. The main failures of the tube hydroforming process, are bursting, wrinkling and buckling. Because of excessive internal pressure in comparison to axial feed, bursting occurs and due to an excessive axial feed with respect to internal pressure, tube fails by wrinkling or buckling [17].

In order to avoid bursting, Oyane's ductile fracture criterion has been employed. In this study, Oyane's ductile fracture criterion is used to predict the forming limit and necking in the tube hydroforming process. This criterion assumes that the history of hydrostatic stress impresses the incidence of the ductile fracture ("Eq. (3)").

$$\int_0^{\bar{\varepsilon}_f} \left(\frac{\sigma_m}{\bar{\sigma}} + C_1 \right) d\bar{\varepsilon} = C_2 \tag{3}$$

In "Eq. (3)", $\bar{\varepsilon}_f$ is the equivalent fracture strain, σ_m is hydrostatic or mean stress, $\bar{\sigma}$ is the equivalent stress, $\bar{\varepsilon}$ is the equivalent strain and, C_1, C_2 are the material constants. The fracture occurs when the value of the left-hand side of the equation reaches the right-hand side value. Oyane's ductile fracture criterion needs two material constants C_1 and C_2, which can be achieved from the limit strains corresponding to a uniaxial and a plane strain tensile test [19].

Material constants of Oyane's ductile fracture criterion for materials of this study were obtained after some finite element modelings and calculations based on references [19-20] as "Table 6".

Table 5 Material constants of Oyane's ductile fracture criterion

Material	C_1	C_2
Annealed Brass	-0.678	1.014
Copper	-0.881	0.910

Another failure in tube hydroforming process is wrinkling. The critical wrinkling stress is determined quantitatively as:

$$\sigma_{cr} = K \sqrt{\frac{2}{1+\alpha^2+(1-\alpha)^2}} \left(c_1 ln \left(1 - \frac{2u_{z_{cr}}}{L} \right) \right)^n \qquad (4)$$

Where:

$$c_1 = -\sqrt{\frac{2}{3} \left(1 + \frac{(1+\alpha)^2+(2\alpha-1)^2}{(2-\alpha)^2} \right)} \qquad (5)$$

In this equation, K is strength coefficient, α is the ratio of hoop stress to axial stress, u_z is axial displacement, L is element length and n is the strain hardening exponent [21].

In order to prevent the occurrence of one of these failures, two criterions via a VUMAT user material linked with ABAQUS/Explicit, are applied to finite element analysis.

3.3. Objective Functions

The bulge height and whole thickness at the branch top have been chosen as the objective functions in this research. Experiments designed in the above using the Taguchi method, are simulated and objective functions were obtained as "Table 7".

Table 6 Experiments performed by finite element analysis

No.	P1	P2	P3		tS6	tS7	H(mm)	t_min(mm)
1	30	31	32	…….	0.625	0.750	8.360	1.604
2	30	31	32	…….	0.750	0.875	8.385	1.607
3	30	31	32	…….	0.750	0.875	8.250	1.610
4	30	31	32	…….	0.625	0.750	Wrinkled	Wrinkled
5	30	31	32	…….	0.750	0.875	8.380	1.599
6	30	31	32	…….	0.625	0.750	8.405	1.604
7	30	31	32	…….	0.625	0.750	8.419	1.625
8	30	31	32	…….	0.750	0.875	8.107	1.662
9	30	34	34	…….	0.625	0.875	8.388	1.606
10	30	34	34	…….	0.750	0.750	8.383	1.598
11	30	34	34	…….	0.750	0.750	8.503	1.590
12	30	34	34	…….	0.625	0.875	Wrinkled	Wrinkled
				…….				
				…….				
				…….				
				…….				
27	34	34	33	…….	0.625	0.750	8.655	1.551
28	34	34	33	…….	0.750	0.875	Burst	Burst
29	34	34	35	…….	0.625	0.750	Wrinkled	Wrinkled
30	34	34	35	…….	0.750	0.875	8.272	1.620
31	34	34	35		0.750	0.875	8.680	1.553
32	34	34	35		0.625	0.750	Burst	Burst

Regression analysis is used to determine mathematical relation between objective functions and loading parameters. In this paper, with an innovative approach, each loading path that one of the failures, including the bursting and the wrinkling occurred in them, have been deleted from the design of experiments table. Removing of the unsuccessful experiments causes a more accurate and less calculations volume of regression analysis. After eliminating failed loading paths, the objective functions are obtained as:

H = -27.584 + 0.00454 P1 + 0.06111 P2 - 0.01335 P3
- 0.03198 P4 + 0.03000 P5 + 0.01742 P6 + 0.0419 P7
+ 0.8654 P8 - 4.1025 tP1 - 1.2515 tP2 - 0.3307 tP4
+ 0.8871 tP5 - 0.2871 tP6 - 0.1277 tP7 + 1.5769 tP8
- 0.08338 S1 - 0.07871 S2 + 0.04865 S3 - 0.00306 S4
+ 0.09058 S5 - 0.1315 tS1 + 0.2373 tS2 + 0.5007 tS3
- 0.7657 tS5   (6)

t_min = 7.23 - 0.00002 P1 - 0.01162 P2 + 0.00685 P4
+ 0.00913 P5 - 0.00991 P6 + 0.0263 P7 - 0.1679 P8
+ 0.704 tP1 + 0.1766 tP2 - 0.097 tP4 - 0.1382 tP5
- 0.0992 tP6 + 0.0606 tP7 - 0.324 tP8 + 0.00988 S1
+ 0.01515 S2 - 0.00727 S3 - 0.00113 S4 - 0.0188 S5
+ 0.1218 tS1 + 0.0025 tS2 - 0.0758 tS3 + 0.1606 tS5
(7)

By using linear stepwise regression analysis to estimate objective functions, the insignificant parameters have been removed from the above equations. The regression models are computed using the statistical analysis in the Minitab software.

The coefficient of determination for H and t_min objective functions are respectively, 99.98% and 98.26%, so it demonstrated that a strong relationship exists between objective functions and loading parameters.

Figure 5 and Figure 6 are the residual plots versus fitted values for H and t_min objective functions. If the points in these graphs are randomly dispersed around the horizontal axis, a linear regression model is appropriate for the data, otherwise, a non-linear model is more suitable [10]. As can be seen in "Fig. 5 and Fig. 6", a random scattering is depicted in the plots and so the regression models are verified.
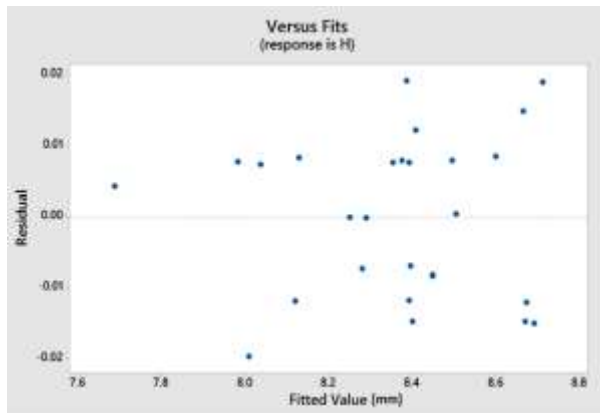

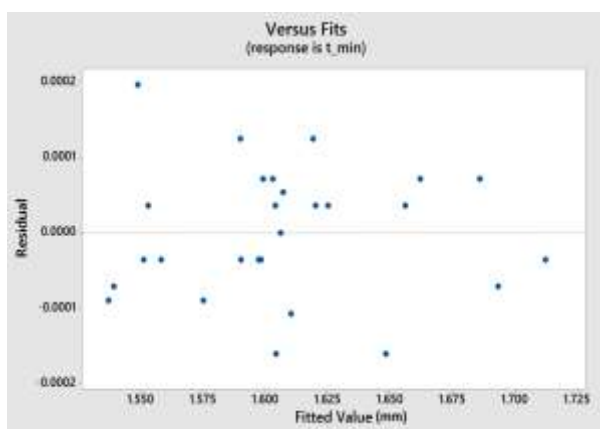**Fig. 5**   Residual plot versus fitted value for H.

Fig. 6   Residual plot versus fitted value for t_min.

3.4. Non-dominated Sorting Genetic Algorithm II (NSGA-II)

One of the most popular multi-objective optimization algorithms is NSGA-II that has three particular features, fast non-dominated sorting approach, fast crowded distance estimation procedure and simple crowded comparison operator. Generally, NSGA-II can be detailed as following steps, (1) Population initialization, (2) Non-dominated sorting, (3) Crowding distance, (4) Selection, (5) Genetic operators and (6) Recombination and selection of new generation [22-23].

In the current study, NSGA-II code has been written in MATLAB software and using it, objective functions are optimized and optimum loading paths have been achieved.

4   RESULTS AND DISCUSSION

Figure 7 illustrates the Pareto optimal front that has been obtained from optimization using NSGA-II.
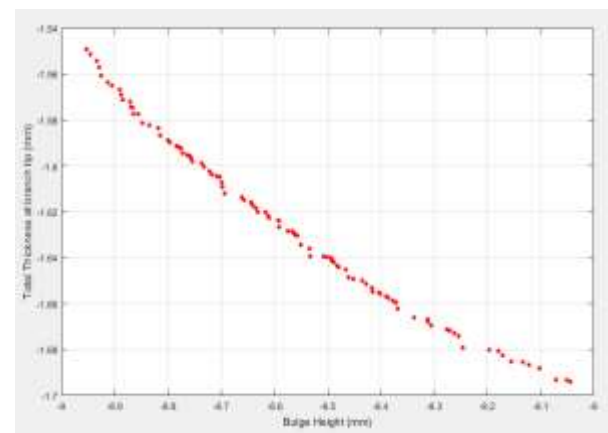

Fig. 7   Pareto optimal front using NSGA-II.

One of the points in the Pareto front has been extracted and loading parameters of that point have been displayed in "Table 8".

Table 7 Optimal results of loading parameters

P1(MPa)	32.2451	tP1(s)	0.0122
P2(MPa)	33.2449	tP2(s)	0.1379
P3(MPa)	32.3915	tP3(s)	0.3002
P4(MPa)	33.5688	tP4(s)	0.3310
P5(MPa)	34.8534	tP5(s)	0.4861
P6(MPa)	35.2848	tP6(s)	0.5608
P7(MPa)	35.9313	tP7(s)	0.7428
P8(MPa)	35.7076	tP8(s)	0.8641
S1(mm)	1.4982	tS1(s)	0.1022
S2(mm)	3.6263	tS2(s)	0.1940
S3(mm)	6.6538	tS3(s)	0.3473
S4(mm)	7.8710	tS4(s)	0.4371
S5(mm)	9.4652	tS5(s)	0.5469
S6(mm)	10.4826	tS6(s)	0.6679
S7(mm)	11.5891	tS7(s)	0.7970

Figure 8 represents the loading path that has been obtained from "Table 8" results.
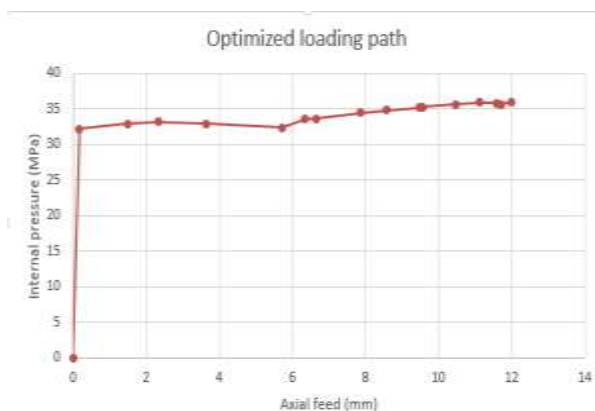
Fig. 8   Optimized loading path.

Figure 9 exhibits equivalent plastic strain of the finite element modeling with the optimized loading path in the above and the bulge height and total thickness in branch tip are respectively, 8.831 mm and 1.583 mm.
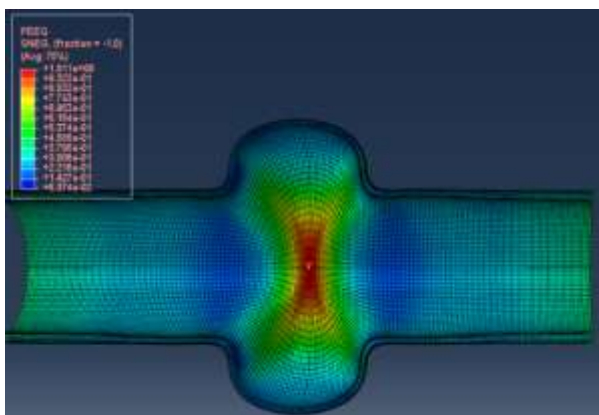

Fig. 9   Finite elements results with optimized loading path.

5   CONCLUSION

In this research, at first a finite element model was performed for double-layered X-shape tube hydroforming using ABAQUS/Explicit and the numerical results were compared with the available experimental results and a good agreement had been observed. In the following, using the design of experiments, initial loading paths was designed and then with regression analysis, a mathematical relation between objective functions and loading parameters was created.

Finally, the objective functions were optimized using non-dominated sorting genetic algorithm II (NSGA-II). Optimum loading path was applied to the finite element model and a better formability (3.4% increase in the bulge height) had been achieved in the results. However, verification of the optimum load path by performing experiments still needs to be done, which is an issue to

consider in the future. Nevertheless, the present results show a qualitative agreement with experiences in practice, see for example [6], [8], [24-25].

REFERENCES

[1] Alaswad, A., Benyounis, K. Y., and Olabi, A. G., Tube Hydroforming Process: A Reference Guide, Journal of Materials and Design, Vol. 33, 2012, pp. 328-339.

[2] Ahmetoglu, M., Altan, T., Tube Hydroforming: State-of-the-Art and Future Trends, Journal of Materials Processing Technology, Vol. 98, No. 1, 2000, pp. 25-33.

[3] Hashemi, R., Faraji, G., Abrinia, K., and Dizaji, A. F., Application of the Hydroforming Strain-and Stress-Limit Diagrams to Predict Necking in Metal Bellows Forming Process, The International Journal of Advanced Manufacturing Technology, Vol. 46, No. 5, 2010, pp. 551-561.

[4] Huang, T., Song, X., and Liu, M., The Multi-Objective Optimization of the Loading Paths for T-Shape Tube Hydroforming Using Adaptive Support Vector Regression, The International Journal of Advanced Manufacturing Technology, Vol. 88, No. 9, 2017, pp. 3447-3458.

[5] Liu, F., Zheng, J., Xu, P., Xu, M., and Zhu, G., Forming Mechanism of Double-Layered Tubes by Internal Hydraulic Expansion, International Journal of Pressure Vessels and Piping, Vol. 81, No. 7, 2004, pp. 625-633.

[6] Wang, X., Li, P., and Wang, R., Study on Hydro-Forming Technology of Manufacturing Bimetallic CRA-Lined Pipe, International Journal of Machine Tools and Manufacture, Vol. 45, No. 4, 2005, pp. 373-378.

[7] Yingyot, A., Gracious, N., and Altan, T., Optimizing Tube Hydroforming Using Process Simulation and Experimental Verification, Journal of Materials Processing Technology, Vol. 146, No. 1, 2004, pp. 137-143.

[8] Aydemir, A., De Vree, J. H. P., Brekelmans, W. A. M., Geers, M. G. D., Sillekens, W. H., and Werkhoven, R. J., An Adaptive Simulation Approach Designed for Tube Hydroforming Processes, Journal of Materials Processing Technology, Vol. 159, No. 3, 2005, pp. 303-310.

[9] Ingarao, G., Di Lorenzo, R., and Micari, F., Internal Pressure and Counterpunch Action Design in Y-Shaped Tube Hydroforming Processes: A Multi-Objective Optimisation Approach, Computers and Structures, Vol. 87, No. 9, 2009, pp. 591-602.

[10] Abedrabbo, N., Worswick, M., Mayer, R., and Van Riemsdijk, I., Optimization Methods for the Tube Hydroforming Process Applied to Advanced High-Strength Steels with Experimental Verification, Journal of Materials Processing Technology, Vol. 209, No. 1, 2009, pp. 110-123.

[11] Di Lorenzo, R., Ingarao, G., and Chinesta, F., Integration of Gradient Based and Response Surface Methods to

Develop a Cascade Optimisation Strategy for Y-Shaped Tube Hydroforming Process Design, Advances in Engineering Software, Vol. 41, No. 2, 2010, pp. 336-348.

[12] Kadkhodayan, M., Erfani Moghadam, A., Optimization of Load Paths in X- and Y-Shaped Hydroforming, International Journal of Material Forming, Vol. 6, No. 1, 2013, pp. 75-91.

[13] Shu-hui, L., Bing, Y., Wei-gang, Z., and Zhong-qin, L., Loading Path Prediction for Tube Hydroforming Process Using a Fuzzy Control Strategy, Materials and Design, Vol. 29, No. 6, 2008, pp. 1110-1116.

[14] Mirzaali, M., Seyedkashi, S. M. H., Liagha.t G. H., Moslmi Naeini, H., Shojaee, G., and Moon, Y. H., Application of Simulated Annealing Method to Pressure and Force Loading Optimization in Tube Hydroforming Process, International Journal of Mechanical Sciences, Vol. 55, No. 1, 2012, pp. 78-84.

[15] Ge, Y., Li, X., Lang, L., and Ruan, S., Optimized Design of Tube Hydroforming Loading Path Using Multi-Objective Differential Evolution, The International Journal of Advanced Manufacturing Technology, Vol. 88, No. 1, 2017, pp. 837-846.

[16] Alaswad, A., Benyounis, K. Y., and Olabi, A. G., Employment of Finite Element Analysis and Response Surface Methodology to Investigate the geometrical factors in T-type Bi-Layered Tube Hydroforming, Advances in Engineering Software, Vol. 42, No. 11, 2011, pp. 917-926.

[17] Olabi, A. G., Alaswad, A., Experimental and Finite Element Investigation of Formability and Failures in Bi-Layered Tube Hydroforming, Advances in Engineering Software, Vol. 42, No. 10, 2011, pp. 815-820.

[18] Shinde, R. A., Patil, B. T., and Joshi, K. N., Optimization of Tube Hydroforming Process (without Axial Feed) by Using FEA Simulations, Procedia Technology, Vol. 23, 2016, pp. 398-405.

[19] Kim, J., Kang, S., and Kang, B., A Prediction of Bursting Failure in Tube Hydroforming Processes Based on Ductile Fracture Criterion, The International Journal of Advanced Manufacturing Technology, Vol. 22, No. 5, 2003, pp. 357-362.

[20] Mahboubkhah, M., Determination of the Forming Limit Ddiagrams by Using the Fem and Experimental Method, Journal of Mechanical Science and Technology, Vol. 27, No. 5, 2013, pp. 1437-1442.

[21] Liu, G., Peng, J., Yuan, S., Teng, B., and Li, K., Analysis on Critical Conditions of Sidewall Wrinkling for Hydroforming of Thin-Walled Tee-Joint, International Journal of Machine Tools & Manufacture, Vol. 97, 2015, pp. 42-49.

[22] Yusoff, Y., Ngaiman, M. S., and Zain, A. M., Overview of NSGA-II for Optimizing Machining Process Parameters, Procedia Engineering, Vol. 15, 2011, pp. 3978-3983.

[23] Torabi, S. H. R., Alibabaei, S., Barooghi Bonab, B., Sadeghi, M. H., and Faraji, G., Design and Optimization of Turbine Blade Preform Forging Using RSM and NSGA II, Journal of Intelligent Manufacturing, Vol. 28, No. 6, 2017, pp. 1409-1419.

[24] Hashemi, R., Assempour, A., Khalil Abad, E. M., Implementation of the Forming Limit Stress Diagram to Obtain Suitable Load Path in Tube Hydroforming Considering M–K Model, Materials & Design, Vol. 30, No. 9, 2009, pp. 3545-3553.

[25] Khalil Abad, E. M., Ghazanfari, A., Hashemi, R., Loading Path Determination for Tube Hydroforming Process of Automotive Component Using APDL, International Journal of Automotive Engineering, Vol. 3, No. 4, 2013, pp. 555-563.